Syndiotactic Polypropylene/Microfibrous Cellulose Composites: Effect of Filler Size on Tensile Properties

Kensuke Miyazaki,[1] Masato Hamadate,[1] Minoru Terano,[2] Hisayuki Nakatani[1]

[1]Department of Biotechnology and Environmental Chemistry, Kitami Institute of Technology 165 Koen-cho, Kitami, Hokkaido, 090-8507, Japan

[2]School of Materials Science, Japan Advanced Institute of Science and Technology, 1-1 Asahidai, Nomi, Ishikawa, 923-1292, Japan

Correspondence to: H. Nakatani (E-mail: nakatani@chem.kitami-it.ac.jp)

ABSTRACT: Syndiotactic polypropylene (SPP)/ethanol swelled microfibrous cellulose (MFC) composite was prepared by a melting mixer, and its morphology and tensile properties were studied. The scanning electron microscope microphotograph did not show the aggregated MFC part up to the 40 wt % MFC loading content, and the Young's modulus was exponentially increasing with the increase of the MFC loading content. These results suggested that the MFC was well-dispersed in the SPP matrix by an ethanol surfactant work. The Young's modulus was much higher than that of the composite with commonly used fibrous cellulose and moreover, exceeded the theoretical one obtained from the Halpin-Tsai equation. The differential scanning calorimetry and wide-angle X-ray diffraction measurements showed that the MFC acted as a good α-nucleation agent for SPP. It was found that the excessive Young's modulus of the MFC composite was originated from an increase of that of the SPP matrix induced by the α-nucleation effect. © 2012 Wiley Periodicals, Inc. J. Appl. Polym. Sci. 000: 000–000, 2012

INTRODUCTION

Cellulose has been one of most popular polymeric materials in the world and is much attractive in low cost, high modulus, renewable, and biodegradability. The structure of cellulose is a branched linear polymer with a high degree of hydrogen bonding.[1] The crystal structure is mainly composed of cellulose-I crystal form with a parallel conformation of two anyhydroglucose units joined by a single β-D glycosidic linkage.[2] Some work has also found that cellulose-I is composed of a mixture of two crystal forms, namely cellulose-I-α and -I-β.[3,4] The crystal deformation behavior has been studied with compacted specimens of a large number of microcrystalline cellulose particles.[5,6] Commercially, cellulose has attracted much attention as filler material because of its high-modulus.[7–25] The composite brings about the improvement of stiffness for pristine polymer. Recently, micro- and/or nano-sized cellulose such as microfibrous cellulose (MFC) and cellulose whisker has been studied as the new filler material by many investigators.[17–25] The micro (nano) cellulose filler has an ability to produce the composite with a higher modulus and/or good transparency. In fact, cellulose is hydrophilic and tends to aggregate in hydrophobic polymer such as polypropylene (PP), causing poor processability and incompatibility. It is very difficult to prepare the compatible micro cellulose composite. Therefore, systematic studies on the physical properties of the micro cellulose composite has been hardly performed.

The purpose of this study is to prepare a compatible polyolefin/MFC composite and to study the dependence of tensile properties on the MFC loading content. Syndiotactic polypropylene (SPP) was used as the polyolefin material as it had good processability at a low temperature (150°C)[26,27] without occurrence of cellulose thermal degradation. However, a novel dispersion method has been required to obtain SPP/MFC composite with good MFC dispersity because of the difference of polarity between both components. In order to prepare the compatible composite, ethanol has been used as surfactant. The MFC dispersity was evaluated by scanning electron microscope (SEM) measurement. The tensile properties were studied in comparison with those of the fibrous cellulose (FC) composite and of the theoretical value obtained from the Halpin-Tsai equation. In addition, the MFC loading effects on the crystallization and crystal morphology were studied by differential scanning

Additional Supporting Information may be found in the online version of this article.

calorimetry (DSC) and wide-angle X-ray diffraction (WAXD) measurements.

EXPERIMENTAL

Materials

SPP was supplied by Sanwayuka Industry Co. The trade name is TOTAL 1751. The number-average molecular weight (M_n) and the polydispersity (M_w/M_n) were 3.5×10^4 and 3.0, respectively. MFC (KY-100 G: solid paste state (dried MFC/water = 10 wt %/90 wt %)) was purchased from Daicel FineChen Ltd. The fiber diameter of the MFC is 10–100 nm (see Figure 1). The length is about 1–10 μm. FC (W-100GK) was donated by Nippon Paper Chemicals. The FC was dried in desiccator for 7 days before preparation. The moisture of the FC was below 0.7 wt %. The FC dimensions are over 90 wt % pass 100 mesh (below 150 μm), the average length was about 37 μm. Ethanol was purchased from Wako Pure Chemical Industry, respectively.

Preparations of MFC Samples

Two kinds of the MFC were used in this study. They were named as "MFC" and "ethanol swelled MFC," respectively. The MFC (KY-100 G) was solid paste containing water as mentioned above. The preparation of the ethanol swelled MFC was as follows: The MFC was poured into a lot of ethanol solvent and was vigorously stirred. The MFC exchanged was separated from ethanol solvent by a suction filtration and was in a solid paste state (MFC/ethanol = 10 wt %/90 wt %). The ethanol swelled paste was used as "ethanol swelled MFC" in this study.

Preparation of Composites

Composites are prepared by an Imoto Seisakusyo IMC-1884 melting mixer. All mixtures (total weight 5 g) were carried by each weight ratio. After a small amount of phenolic antioxidant (Adekastab AO-60, ca. 0.5%) was added, the mixing was performed at 150°C at 60 rpm for 5 min except the SPP/ethanol swelled MFC composite. In the case of the SPP/ethanol swelled MFC composite, the mixing was performed at 165°C at 60 rpm for 10 min because the ethanol volatilization brought about the decrease of the mixing temperature. First, the SPP was put into
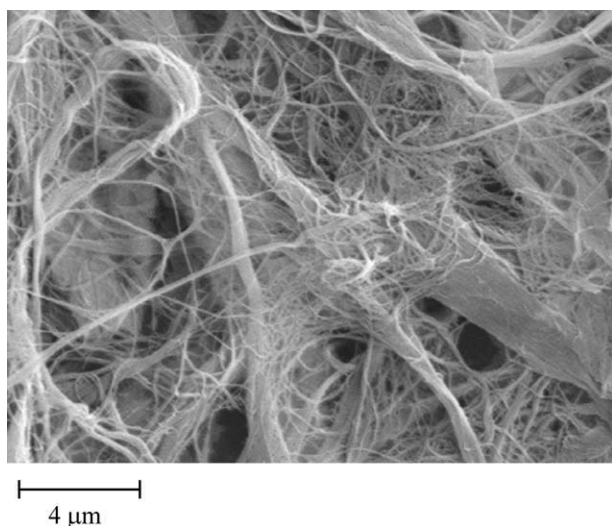

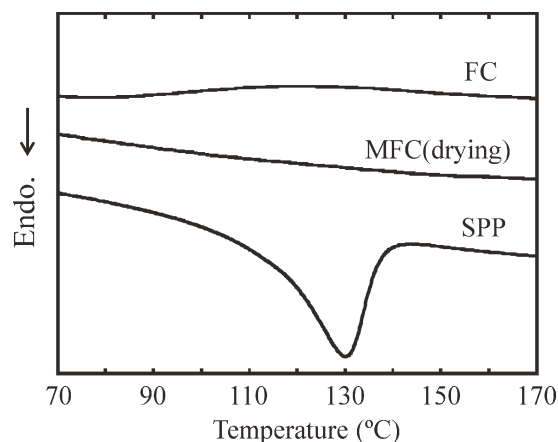**Figure 1.** SEM microphotograph of MFC.

Figure 2. DSC curves of heating scans for SPP, MFC(drying), and FC.

the melting mixer, and then the MFC ethanol solid paste was added with letting the ethanol vapor out. The composites obtained were molded into the film (100 μm) by compression molding at 150°C under 40 MPa for 5 min.

Scanning Electron Microscope Observation

SEM observation was carried out with a JEOL JSM-5800 at 20 kV. The composite was molded into the plate (ca.500 μm) by compression molding at 150°C under 40 MPa for 5 min. The plate obtained was fractured in liquid nitrogen, was trimmed by a microtome, and then the fractured surface was sputter-coated with gold.

Differential Scanning Calorimetry Measurement

DSC measurements were made with a Shimadzu DSC-60. The film (thickness: 100 μm) samples of about 2 mg weight were sealed in aluminum pans. The measurements of the samples were carried out at heating and cooling rates of 10°C/min under a nitrogen atmosphere, respectively. From the thermogram, melting temperature (T_m) and fusion enthalpy (ΔH) were determined. The crystallinity (X_c) of the SPP part in the composite was obtained by using the relationship:[28]

$$X_c = (\Delta H/\Delta H^\circ) \cdot (100/w) \qquad (1)$$

where $\Delta H^\circ = 109.3$ J/g for 100% crystalline SPP was taken,[29] and w is the mass fraction of SPP in the composite.

Wide-Angle X-Ray Diffraction Measurement

WAXD diffractograms were recorded in reflection geometry at 2° (2 theta/min) under Ni-filtered Cu Ka radiation using a RIGAKUXG-RINT 1200 diffractometer. The MFC was molded into the film (100 μm) by compression molding at r.t. under 5 MPa for 7 min and then sufficiently dried at r.t. In the case of FC sample, the FC was sufficiently dried at r.t. without compression molding. They were measured by the WAXD device. These crystallinity values were estimated from the WAXD profiles according to Ant-Wuorinen's report.[30] The WAXD measurement of the composite was carried out with the 100 μm film.
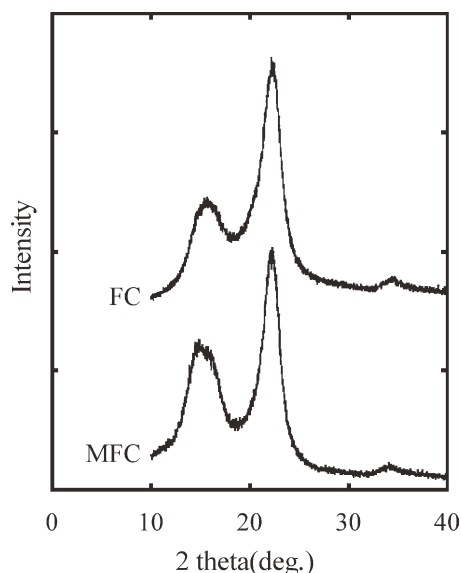
Figure 3. WAXD profiles of MFC and FC.

Figure 4. SEM microphotographs of the surfaces of the SPP(98 wt %)/ water swelled MFC(2 wt %).

Tensile Testing

Stress-strain behavior was observed using a SHIMADZU EZ-S at a cross-head speed of 3 mm/min. The sample specimens were cut with dimensions 30 × 5 × 0.1 mm shape in which the gage length was 10 mm. We chose the specialized specimen (like ISO reed-shape) to adapt to the size of our tensile testing machine. All of tensile testing were performed at 20°C. The values of Young's modulus were obtained from the tangent slope of the stress-strain curve (until about 1% of the strain value). All results obtained were the average values of ten measurements.
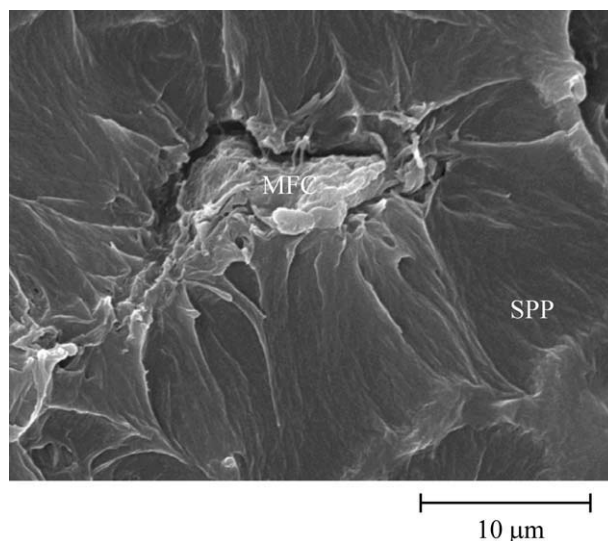
RESULTS AND DISCUSSION

Figure 2 showed the DSC curves of the SPP, MFC, and FC. The SPP melting temperature (T_m) is 130°C, and the other materials have no T_m. All materials have no exothermal peaks, showing pyrolysis does not occur up to 170°C. These results indicate that thermal deterioration of the cellulose materials does not occur under the composite preparation process. Figure 3 showed the WAXD profiles of the MFC and FC. Both of them show typical cellulose-I crystal form,[31] and their crystallinity values of the MFC and the FC are 62% and 53%, respectively.
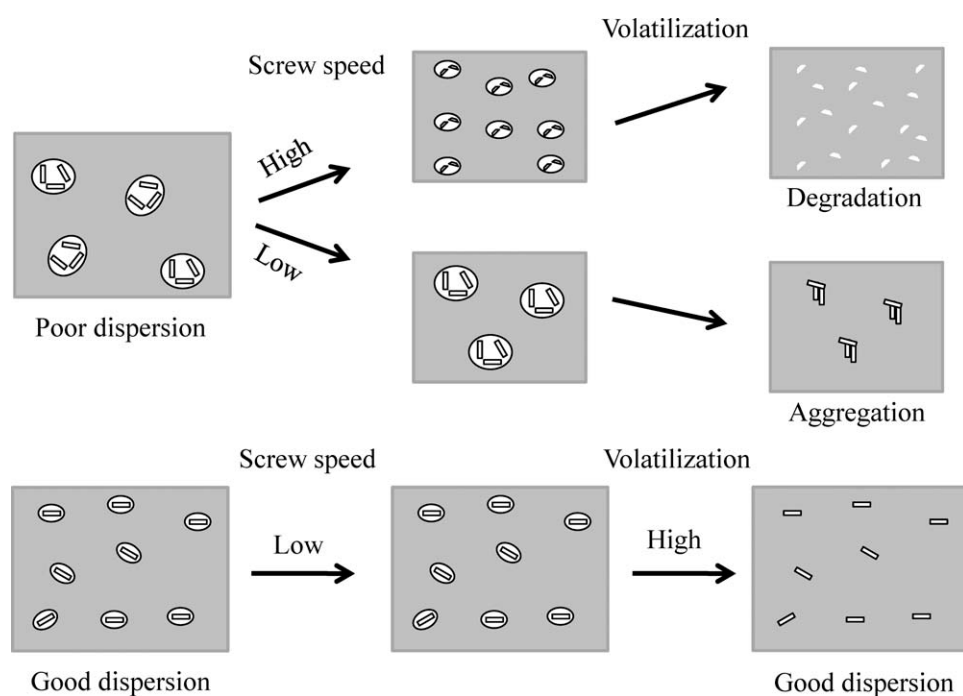

Figure 5. Plausible mechanism of MFC dispersion in polyolefin using various lubricants.
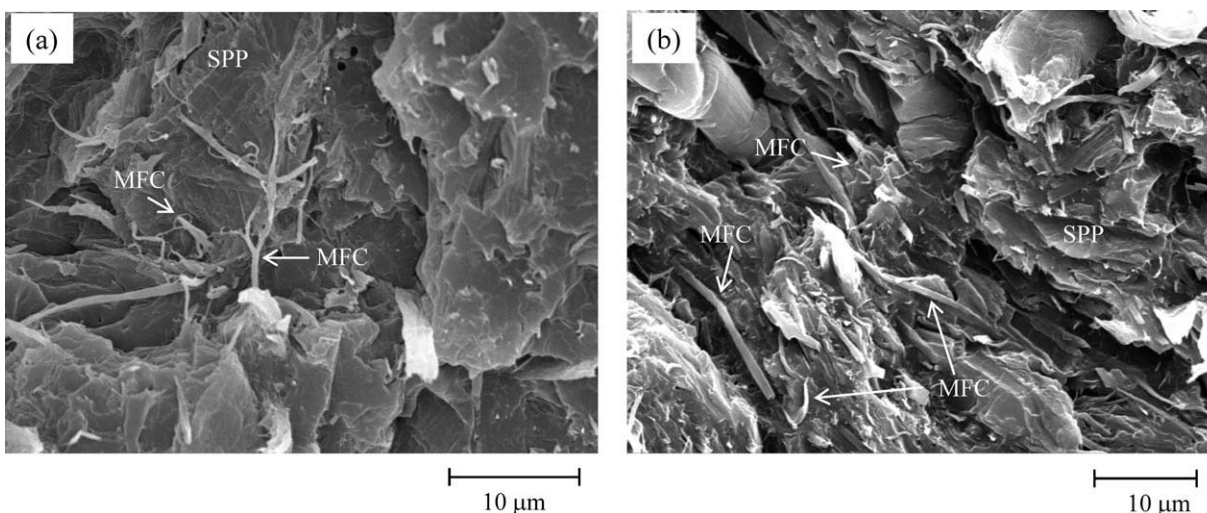
Figure 6. SEM microphotographs of the surfaces of the SPP/ethanol swelled MFC. (a): SPP (80 wt %)/ethanol swelled (20 wt %). (b): SPP (60 wt %)/ethanol swelled (40 wt %).

Figure 4 showed the SEM micrograph of the SPP(98 wt %)/MFC(2 wt %) surface. An aggregated MFC (ca. 15 μm) can be also observed, and the interface between the MFC and SPP matrix is defined. In the melt mixing process, the presence of water acts as a lubricant and supports the MFC dispersion.[20] In this work, the effect is less due to the low screw speed (60 rpm). The water lubricant method requires high screw speed to obtain good MFC dispersity in polyolefin matrix such as polyethylene.[20] As shown in Figure 5, the requirement is due to low solubility of water against polyolefin, and the water lubricant brings about a phase separation structure in this melt mixing process. The water domain size certainly depends on the magnitude of shear stress produced by the screw. The larger domain includes many MFCs. After the water vaporization in the melt mixing process, the aggregated MFCs are left at the imprint of the domain, leading to the lower dispersity. Although the higher screw speed is desirable in terms of dispersity, it simultaneously brings about thermal deterioration of MFC.[20] As another method to get the good MFC dispersity, there is a surfactant application. Ljungberg et al. reported that phosphoric ester of

polyoxyethylene-9-nonylphenyl ether (BNA) was useful as a surfactant to prepare PP/MFC composite showing a good MFC dispersity.[18,19] The BNA surfactant can bring about the good MFC dispersity even by cast film methods,[18,19] suggesting that it has an ability to produce the SPP/MFC composite with a well-dispersed MFC even at the low screw speed. However, the BNA with such molecular weight would certainly remain in the SPP/MFC composite and would affect the properties.[19] It is inappropriate to add much amount of such surfactant into the SPP/MFC composite in terms of the properties such as tensile one.

A surfactant showing high volatility must be required to prepare the SPP/MFC composite with a high MFC content at low screw speed. As such surfactant, ethanol is considered because it is compatible for both of water and hydrocarbon and has a low boiling point (80°C) required for rapid volatilization. As shown in Figure 5, the application of the MFC ethanol solid paste has a potential for providing the good dispersity in the SPP matrix even at low screw speed. Figure 6 showed the SEM microphotographs of the surfaces of the SPP (80 wt %)/ethanol swelled
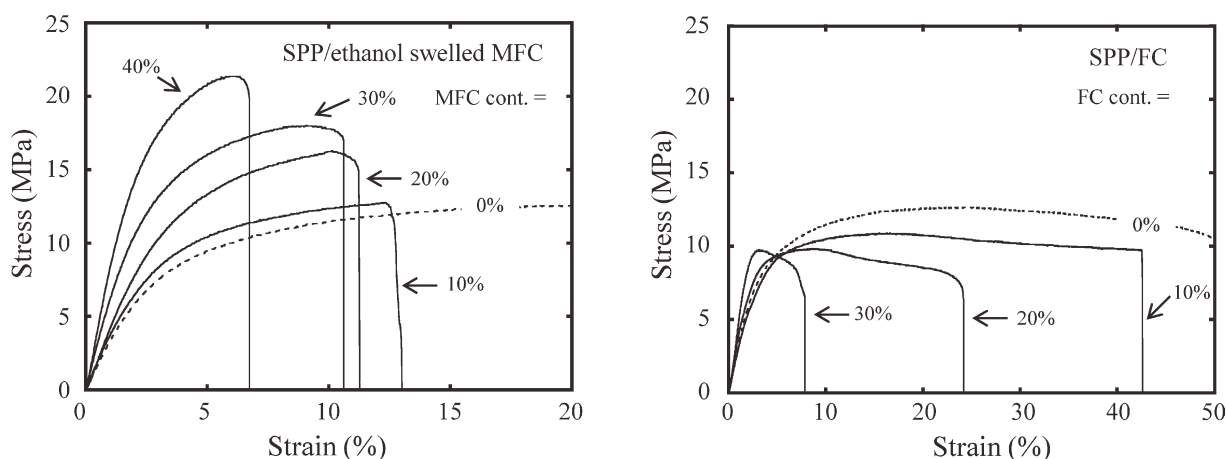

Figure 7. Stress-strain curves of SPP/ethanol swelled MFC and SPP/FC composites with various cellulose filler content.
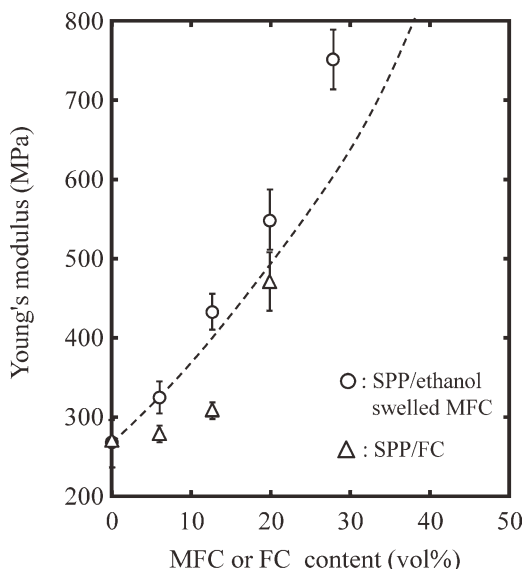
Figure 8. Young's modulus of SPP composite against MFC or FC content (vol %). Broken curve: The Halpin-Tsai equation. MFC or FC = 10, 20, 30, and 40 wt % corresponding to = 6.1, 12.7, 19.9, and 27.9 vol %, respectively. Preparation of SPP (60 wt %)/FC (40 wt %) composite was impossible.

MFC (20 wt %) and SPP (60 wt %)/ethanol swelled MFC (40 wt %). The aggregated MFC parts are not observed in both of the microphotographs. These results suggest that ethanol acts as a good surfactant for MFC.

All of the stress-strain curves of the SPP/ethanol swelled MFC and SPP/FC composites were plotted in Figure 7. Figure 8 showed the plot of Young's modulus versus MFC or FC content (vol %) for the SPP composites. The Young's moduli of both of the SPP composites are increasing with the increase of the MFC or FC content. The effect of the MFC loading on the Young's modulus is higher than that of the FC one, and the values of the 6.1 vol % (10 wt %), 12.7 vol %(20 wt %) and (30 wt %) MFC content are 117, 140, and 117% higher than those of the FC, respectively. Effect of filler material on Young's modulus can be estmated by the Halpin-Tsai equation.[32–34]

$$M = M_1 \frac{1 + AB\phi}{1 - AB\phi} \quad (2)$$

in which

$$A = k_E - 1 \quad (3)$$

$$B = \frac{(M_2/M_1) - 1}{(M_2/M_1) + A} \quad (4)$$

where M, M_1, and M_2 are moduli of the composite, SPP matrix, and MFC or FC filler component, respectively; ϕ is the volume fraction (vol %) of component; k_E is the Einstein coefficient; A is the transference efficiency from the matrix to the filler. The M_1 (268 MPa) was directly obtained from the SPP sample, and the M_2 (9.2 GPa) was assumed as Young's modulus of
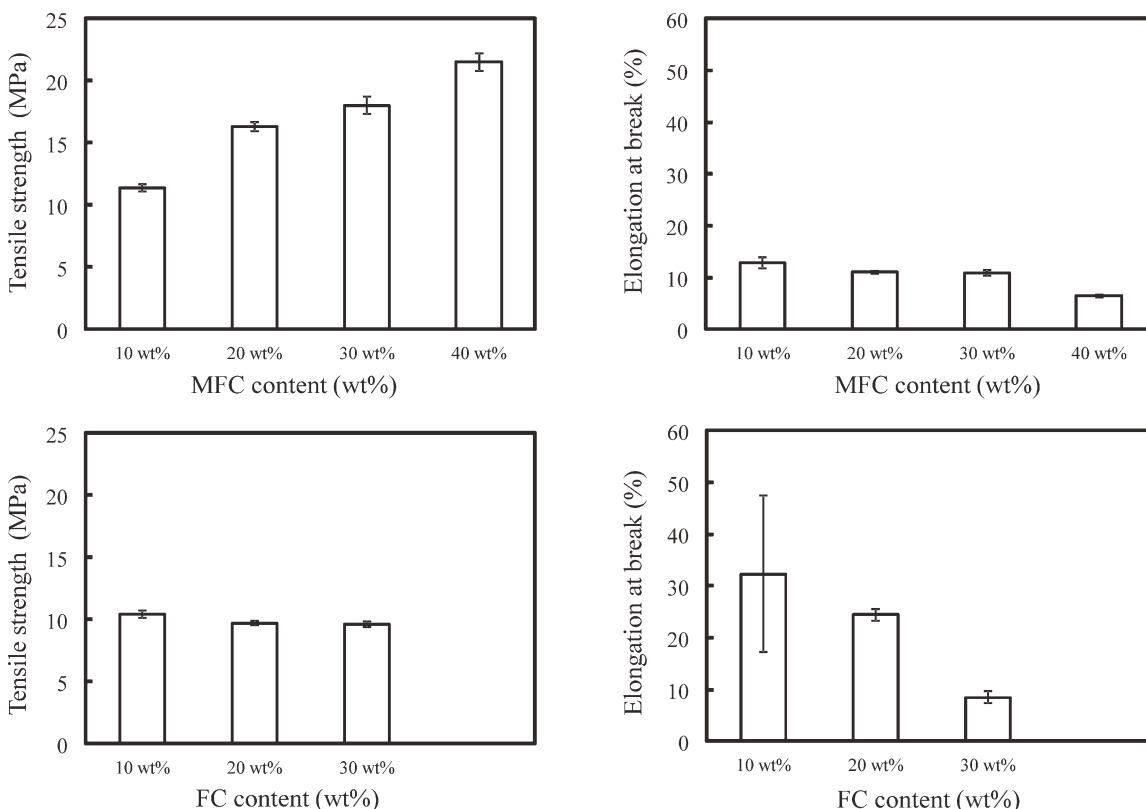

Figure 9. Comparisons of tensile strengths and elongations at break of SPP/ethanol swelled MFC and SPP/FC composites with various cellulose filler content. The elongation at break of the SPP is 200% over. Preparation of SPP (60 wt %)/FC (40 wt %) composite was impossible.
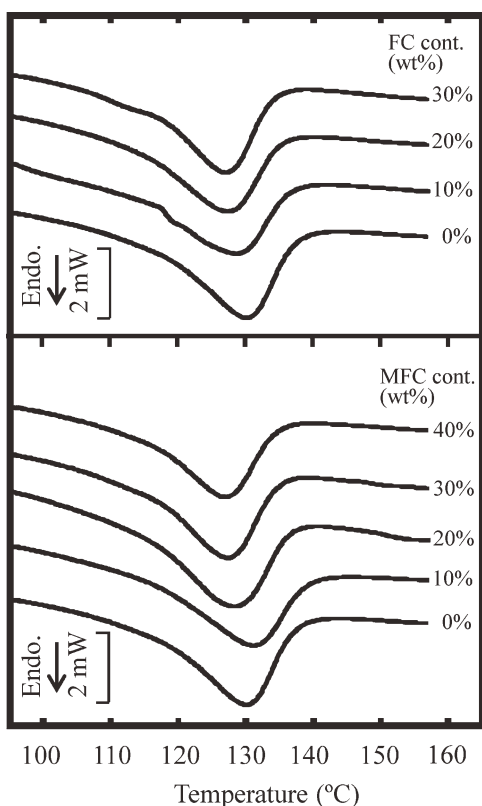
Figure 10. DSC curves of heating scans for SPP/FC (top) and SPP/ethanol swelled MFC (bottom) composites. The numeric characters on the curves are FC or MFC wt % in composites. The endothermal peaks are corresponding to melting temperatures (T_m).

Figure 11. DSC curves of cooling scans for SPP/FC (top) and SPP/ethanol swelled MFC (bottom) composites. The numeric characters on the curves are FC or MFC wt % in composites. The exothermal peaks are corresponding to crystallization temperatures (T_c).

microcrystalline cellulose.[6] k_E has a strong correlation with Poisson's ratio v. v of composite is approximately given by a mixture rule:[35]

$$v = v_m \phi_m + v_f \phi_f \quad (5)$$

where v_m and v_f are the Poisson's ratios of matrix (SPP) and filler (MFC or FC), respectively; ϕ_m and ϕ_f are the volume fractions of matrix and filler, respectively. The Poisson's ratios used in this approach having the following values: $v_m = 0.38$[36] and $v_f = 0.30$.[36] The v obtained is from 0.36 to 0.38. According to the data of Nielsen,[34] in a rigid matrix having near v value (0.35), the Einstein coefficient k_E was 3.81. Therefore, in this study, the v and the k_E have been regarded as 0.35 and 3.81, respectively, and the values of A and B have been estimated form eqs. (3) and (4). The Halpin-Tsai equation obtained was plotted in Figures 8. Interestingly, the Young's moduli of the SPP/ethanol swelled MFC composites are higher than those of the Halpin-Tsai equation. The values of the 6.1 vol % (10 wt %), 12.7 vol % (20 wt %), 19.9 vol % (30 wt %), and 27.9 vol % (40 wt %) MFC content are 0.9%, 9.3, 12.2, and 23.9% higher than those of the Halpin-Tsai equation, respectively. The gap between the measured and Halpin-Tsai equation values is markedly increased with the increase of the MFC content. In contrast, the Young's moduli of the SPP/FC composites are lower than those of the Halpin-Tsai equation. The difference of the tensile behavior
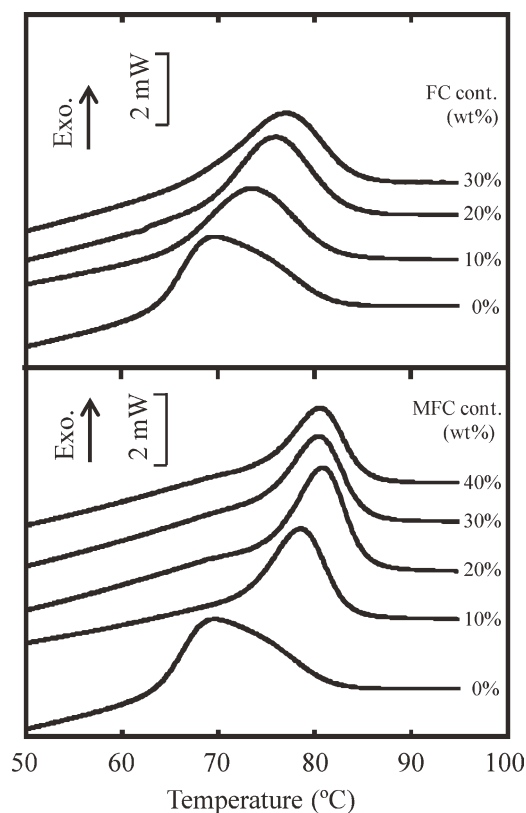
between the MFC and FC composites would be mainly originated from total interface surface area. The total surface area of the MFC is much larger than that of the FC because of the much smaller size (see Experimental section). Therefore, the total friction force acting on the MFC is much larger, and a shear stress from the SPP matrix is efficiently applied to the MFC filler. Figure 9 showed the comparisons of the tensile strengths and elongations at break of the SPP/ethanol swelled MFC and SPP/FC composites with various MFC or FC content. The tensile strength of the SPP/ethanol swelled MFC certainly increases with the increase of the MFC content, and the dependence of the elongation at break on the MFC content is less. It seems that the interfacial defect such as void is hard to produce. In contrast, the dependence of the tensile strength on the FC content is less, and the elongation at break rapidly decreases with increase of the FC content. The behavior suggests that the shear stress from the SPP matrix is inefficiently applied to the FC by blocking of the interfacial defect such as void. In fact, the SEM microphotograph of the SPP/FC showed that a large void existed between the FC and the SPP matrix. When the tensile stress is applied to the SPP/FC, the transmission of the applied stress is prevented by the void. The elongations at break of the 10 wt % and 20 wt % FC content are 32.3 ± 15.1% and 24.4 ± 1.2%, respectively and are considerably higher than those of the MFC composites with the same content. The deformation of only the SPP matrix occurs during the tensile testing

Table I. Melting Temperature (T_m), Fusion Enthalpy (ΔH), Crystallinity (X_c), and Crystallization Temperature (T_c) of SPP/Ethanol Swelled MFC and SPP/FC Composites

MFC or FC cont. (wt %)	T_m (°C)	ΔH (J/g)	X_c (%)*	T_c (°C)
MFC				
0	130	24.4	22	69
10	131	22.9	23	78
20	128	27.3	31	81
30	127	25.1	33	81
40	127	20.4	31	81
FC				
10	129	24.3	25	74
20	127	23.2	27	76
30	127	24.1	32	77

*X_c was obtained from eq. (1) (see Experimental Part).

in the SPP/FC, resulting that the SPP/FC shows the much greater elongation.

The Young's moduli of the SPP/ethanol swelled MFC composites exceed the theoretical ones obtained from the Halpin-Tsai equation. The phenomenon would be explainable in terms of an increase of the Young's modulus of the SPP matrix. Figures 10 and 11 showed the DSC curves around the melting (T_m) and crystallization (T_c) temperatures, respectively. These results were summarized in Table I. The T_m values are lowered from 130°C to 127°C. The declining trend in T_m is exhibited up to the 20 wt % MFC or FC content, and then their T_m values are almost constant at 130°C. Interestingly, there is a difference between the ethanol swelled MFC and FC composites in the content dependence of the crystallinity (X_c). The X_c of the ethanol swelled MFC composite rapidly increases up to the 20 wt % content and then is saturated at about 31%. The T_c increasing tendency is similar to that of the X_c. The Young's modulus gap between the measured and Halpin-Tsai equation values is markedly increased with the increase of the MFC content. The X_c increment leads to an increase of the Young's modulus of the SPP matrix itself, causing the excessive increase of that of the SPP/ethanol swelled MFC composite. It is well known that crystallinity and crystallization rate of polymer materials increase with nucleating agent effect.[28,37–39] Therefore, the X_c and T_c increment indicates that the MFC certainly acts as a nucleating agent for SPP. There is an interaction between cellulose and isotactic polypropylene (IPP) at a molecular level.[38] Cellulose surface has many the α-nucleation sites formed by the interaction, resulting that the IPP transcrystallization occurs.[38] It seems that the interaction acts as the α-nucleation site for the crystallization in SPP as well as IPP.[28] In particular, the MFC has a good ability to act as the α-nucleation agent because of its large total surface area. As shown in Figure 12, the main peaks corresponding to SPP crystal form in the profiles of the SPP/ethanol swelled MFC composites are at $2\theta = 12.2°$, $15.9°$, and $20.6°$ (corresponding to orthorhombic α-form (Form I)),[40] respectively, and their peak location coincides with that of the pristine SPP. The

WAXD profiles suggest that the MFC has only the α-nucleating effect on SPP. The MFC existence induces the α-form crystallization of a less crystallizable part in the SPP matrix, resulting that the SPP crystals with a lower degree of perfection, i.e., thicker lamellar, is produced. The apparent T_m shifts to a lower temperature by the increase in population of such SPP crystals. A degree of lowering of the apparent T_m reflects the α-nucleating effect. The α-nucleation effect such as the X_c and T_c increment is saturated over the 20 wt % MFC loading content. The saturation behavior is originated from the microstructured (nanostructured) cellulose surface since the FC with less total surface area does not show it. The population of the α-nucleation site at the 20 wt % MFC content reaches a concentration sufficient to crystallize all of crystallizable SPP part. The higher deviation from the Halpin-Tsai equation is originated from the Young's modulus change of the SPP matrix induced by the crystallinity change from 22% to 31%. It is found that the loading of the MFC brings about the Young's modulus improvement of the SPP with both of the higher modulus of MFC itself and the α-nucleating effect for the matrix.

CONCLUSIONS

The morphology and tensile properties of the SPP/ethanol swelled MFC composite were studied as compared with those of the SPP/FC one. The aggregated MFC part was not observed in the SEM microphotographs, and the Young's modulus of the composite was exponentially increasing with the increase of the MFC content. These results suggested that the MFC was well-dispersed in the SPP matrix by ethanol surfactant. The effect of the MFC loading on the Young's modulus was much higher than that of the FC one. The Young's modulus of the SPP/
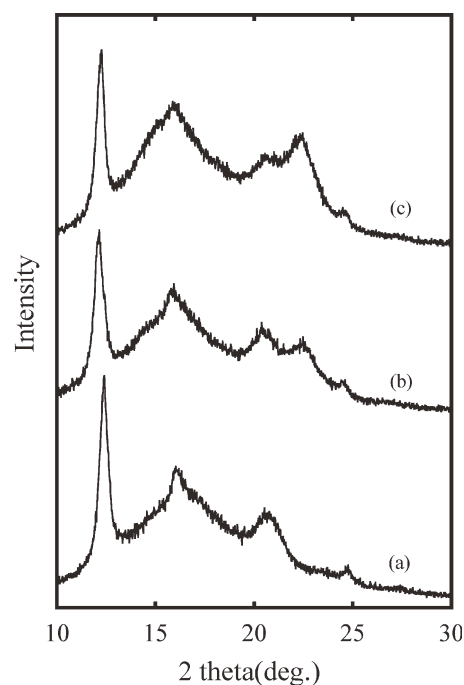

Figure 12. WAXD profiles of SPP and SPP/ethanol swelled MFC composites. (a): SPP. (b): SPP (80 wt %)/ethanol swelled (20 wt %). (c): SPP (60 wt %)/ethanol swelled (40 wt %).

ethanol swelled MFC composite exceeded the theoretical one obtained from the Halpin-Tsai equation. The MFC acted as a good α-nucleation agent for SPP because of its large total surface area. The excessive Young's modulus of the MFC composite was originated from an increase of that of the SPP matrix induced by the α-nucleation effect.

REFERENCES

1. Eichhorn, S. J.; Young, R. J. *Cellulose* **2001,** *8*, 197.
2. Marchessault, R. H.; Sundararajan, P. R. The Polysaccharides, Cellulose, Aspinall G. O., Eds.; Academic Press: New York, **1983;** *Vol. 1*, pp 12–90.
3. Atalla, R. H.; Van der Hart, D. L. *Science* **1984,** *223*, 283.
4. Van der Hart, D. L.; Atalla, R. H. *Macromolecules* **1984,** *17*, 1465.
5. Edge, S.; Fraser Steele, D.; Chen, A.; Tobyn, M. J.; Staniforth, J. N. *Int. J. Pharm.* **2000,** *200*, 67.
6. Hancock, B. C.; Clas, S.-D.; Christensen, K. *Int. J. Pharm.* **2000,** *209*, 27.
7. Takase, S.; Shiraishi, N. *J. Appl. Polym. Sci.* **1989,** *37*, 645.
8. Maldas, D.; Kokta, B. V.; Daneault, C. *J. Appl. Polym. Sci.* **1989,** *37*, 751.
9. Raj, R. G.; Kokta, B. V.; Maldas, D.; Daneault, C. *J. Appl. Polym. Sci.* **1989,** *37*, 1089.
10. Hedenberg, P.; Gatenholm, P. *J. Appl. Polym. Sci.* **1996,** *60*, 2377.
11. Zhang, F.; Qiu, W.; Yang, L.; Endo, T. *J. Mater. Chem.* **2002,** *12*, 24.
12. Qiu, W.; Zhang, F.; Endo, T.; Hirotsu, T. *J. Appl. Polym. Sci.* **2003,** *87*, 337.
13. Qiu, W.; Zhang, F.; Endo, T.; Hirotsu, T. *J. Appl. Polym. Sci.* **2004,** *91*, 1703.
14. Felix, J. M.; Gatenholm, P. *J. Appl. Polym. Sci.* **1991,** *42*, 609.
15. Qiu, W.; Zhang, F.; Endo, T.; Hirotsu, T. *J. Appl. Polym. Sci.* **2004,** *94*, 1326.
16. Hristov, V. N.; Vasileva, S. T.; Krumova, M.; Lach, R.; Michler, G. H. *Polym. Compos.* **2004,** *25*, 521.
17. Grunert, M.; Winter, W. T. *J. Polym. Env.* **2002,** *10*, 27.
18. Ljungberg, N.; Bonini, C.; Bortolussi, F.; Boisson, C.; Heux, L.; Cavaillé, J. Y. *Biomacromolecules* **2005,** *6*, 2732.
19. Ljungberg, N.; Cavaillé, J. Y.; Heux, L. *Polymer* **2006,** *47*, 6285.
20. Soulestin, J.; Quiévy, N.; Sclavons, M.; Devaux, J. *Polym. Eng. Sci.* **2007,** *47*, 467.
21. Gray, D. G. *Cellulose* **2008,** *15*, 297.
22. De Menezes, A. J.; Siqueira, G.; Curvelo, A. A. S.; Dufresne, A. *Polymer* **2009,** *50*, 4552.
23. Yang, H. S.; Gardner, D. J.; Nader, J. W. *J. Therm. Anal. Calori* **2011,** *103*, 1007.
24. Yang, H. S.; Gardner, D. *J. Wood Fiber Sci.* **2011,** *43*, 143.
25. Yang, H. S.; Gardner, D. *J. Wood Fiber Sci.* **2011,** *43*, 215.
26. Nakatani, H.; Iwakura, K.; Miyazaki, K.; Okazaki, N.; Terano, M. *J. Appl. Polym. Sci.* **2011,** *119*, 1732.
27. Nakatani, H.; Iwakura, K.; Hamadate, M.; Okazaki, N.; Aoyama, M.; Terano, M. *J. Appl. Polym. Sci.* **2011,** *122*, 2798.
28. Amash, A.; Zugenmaier, P. *Polym. Bull.* **1998,** *40*, 251.
29. Supaphol, P.; Spruiell, J. E.; Lin, J.-S. *Polym. Int.* **2000,** *49*, 1473.
30. Ant-Wuorinen, A. W.; Visapää, A. *Norelco Reptr* **1962,** *9*, 48.
31. Ishikawa, A.; Okano, T.; Sugiyama, J. *Polymer* **1997,** *2*, 463.
32. Halpin, J. C. *J. Compos. Matter* **1969,** *3*, 732.
33. Lewis, T. B.; Nielsen, L. E. *J. Appl. Polym. Sci.* **1970,** *14*, 1449.
34. Nielsen, L. E. *J. Appl. Phys.* **1970,** *41*, 4626.
35. Helbert, W.; Cavaillé, J. Y.; Dufresne, A. *Polym. Compos.* **1996,** *17*, 604.
36. ASP, L. E.; Sjögren, B. A.; Berglund, L. A. *Polym. Compos.* **1997,** *18*, 9.
37. Kaempfer, D.; Thomann, R.; Mülhaupt, R. *Polymer* **2002,** *43*, 2909.
38. Felix, J. M.; Gatenholm, P. *J. Mater. Sci.* **1994,** *29*, 3043.
39. Xua, T.; Lei, H.; Xie, C. S. *Mater. Des.* **2003,** *24*, 227.
40. De Rosa, C.; Auriemma, F.; Vinti, V. *Macromolecules* **1997,** *30*, 4137.